THERMAL-MECHANICAL TEST AND ANALYSIS OF A CARBON-CARBON CONTROL SURFACE

RANDOLPH C. THOMPSON
PRC INC.
P.O. BOX 273, BUILDING 4839
EDWARDS, CALIFORNIA 93523-0273

JAMES WAYNE SAWYER
MS-396
NASA LANGLEY RESEARCH CENTER
HAMPTON, VIRGINIA 23681

ROGER A. FIELDS
NASA DRYDEN FLIGHT RESEARCH FACILITY
P.O. BOX 273, MS-4820-1A
EDWARDS, CALIFORNIA 93523-0273

R. FRANKLIN VAUSE
LOCKHEED ENGINEERING AND SCIENCES CORPORATION
NASA LANGLEY RESEARCH CENTER
HAMPTON, VIRGINIA 23681

ABSTRACT

Mechanical loading tests were performed on a carbon-carbon composite elevon control surface to determine the structural adequacy of this concept for hypersonic flight environments and to compare test data with analysis. This paper describes the test component, the analytical methodology, and the test techniques and setup used to apply the mechanical loads and determine the control surface's response to applied load. The results from the room-temperature mechanical load tests are compared with analytical predictions from finite element analyses. In addition, the planned thermal-mechanical test program is presented and discussed.

NOMENCLATURE

ACC	advanced carbon-carbon
DFRF	Dryden Flight Research Facility, Edwards, CA
DLL	design limit load
EAL	engineering analysis language
LaRC	Langley Research Center, Hampton, VA
NASA	National Aeronautics and Space Administration
NASP	National AeroSpace Plane
SG	strain gage, figure 9
SINDA '85	system improved numerical differencing analyzer
TC	thermocouple
$\mu\varepsilon$	microstrain
μV	microvolt

INTRODUCTION

Advanced carbon-carbon (ACC) composite material has been considered for structural applications on the National AeroSpace Plane (NASP) because of its low density and high strength at elevated temperatures. As part of the NASP Structures Technology Maturation Program, the National Aeronautics and Space Administration's (NASA) Langley Research Center (LaRC) investigated the use of carbon-carbon composite material for control surfaces on the NASP generic vehicle concept. An elevon control surface was selected for a development program and a full-scale segment of a carbon-carbon control surface has been designed and fabricated [1-8]. This full-scale segment is currently undergoing mechanical and thermal-mechanical testing at the NASA Dryden Flight Research Facility (DFRF) Thermostructural Laboratory.

The primary objectives of the carbon-carbon control surface development program are to (1) select a least-weight structural concept for moveable control surfaces that offers adequate life and can sustain the vehicle operating environment, (2) develop the design and fabrication technology for the selected concept, and (3) verify the structural adequacy of the selected concept through coupon, small segment, and full-scale component mechanical and thermal-mechanical testing. Other objectives of the

program are to develop thermoelastic analysis techniques, high-temperature instrumentation and attachment techniques for use on coated carbon-carbon, and high-temperature test techniques for carbon-carbon structures.

The first two primary objectives have been accomplished. Currently, the carbon-carbon control surface is undergoing full-scale thermal-mechanical testing (objective three). Objective three involves room-temperature mechanical load tests as well as a combined thermal and mechanical load test series which will be conducted in several stages with maximum temperatures of 204 °C (400 °F), 427 °C (800 °F), 1038 °C (1900 °F), and 1649 °C (3000 °F) respectively. Each test adds increased complexity to the required test and analytical techniques.

This paper discusses the room-temperature mechanical load evaluation tests performed on the carbon-carbon control surface test component. A description of the test component, the analytical methodology, and the test techniques and setup used to apply the mechanical loads and determine the control surface's response to applied loads, is presented. Results from the room-temperature mechanical load tests are discussed and correlated with analytical predictions from finite element analyses performed at NASA LaRC. The planned thermal-mechanical test program will also be presented and discussed along with some of the challenges associated with the planned high-temperature structural testing.

TEST ARTICLE DESCRIPTION

The carbon-carbon control surface test component is a full-scale segment of an elevon control surface for a NASP generic vehicle (Fig. 1). The control surface measures 98.3 cm (38.7 in.) wide by 142.2 cm (56.0 in.) long and has a maximum thickness of 35.6 cm (14.0 in.) at the root tapering to 16.3 cm (6.4 in.) at the tip. The control surface is a uniquely designed and fabricated test article. It is the first (1) demonstration of a large-scale, designed-to-tolerance, highly loaded carbon-carbon structure, (2) demonstration of co-bonded carbon-carbon structural joints, (3) demonstration of a load carrying carbon-carbon torque tube, and (4) structural application of carbon-carbon fasteners.

An exploded view of the carbon-carbon control surface is shown in Figure 2. The test component consists mostly of ACC parts. There are two rib-stiffened skin panels, a torque tube, ten attachment rings, a close-out channel, and fasteners fabricated from carbon-carbon. There are also two attachment rings, cleats, fasteners, and hinge fittings fabricated from Rene´ 41. The two rib stiffened panels are fabricated from the same tooling and are then joined together by a secondary bonding operation to form the upper and lower skin and rib structure of the elevon. This causes the ribs to be offset and the control surface to be slightly unsymmetric about the vertical mid-plane. All of the carbon-carbon parts have a conversion coating of silicon carbide. Carbon-carbon attachment rings are used to attach the ribs to the torque tube. Rene´ 41 attachment rings are used to attach the torque tube to test support structure which simulates the attachment points on an actual aircraft wing. Carbon-carbon fasteners are used to attach the ribs to the carbon-carbon attachment rings and to provide a back-up to the center co-bonded region of the ribs as an added precaution in the event of bond failure due to thermal or mechanical loads.

Aerodynamic loads acting on the control surface skins are transmitted through the ribs and into the torque tube by the carbon-carbon attachment rings and then into the aircraft by the Rene´ 41 attachment rings. The joint between the carbon-carbon torque tube and the Rene´ 41 attachment rings (Fig. 3) is the most critical area of the design due to the torque loads that must be transferred at those locations. These torque loads are transmitted from the carbon-carbon torque tube to the Rene´ 41 attachment rings by a series of Rene´ 41 rectangular cleats cantilevered from the inside surface of the attachment rings. There are four rows of eight cleats with two rows positioned 19.1 cm (7.5 in.) from each end of the torque tube. The load is transferred from the torque tube to the cleats through the bearing surfaces between the cleats and torque tube. This load transfer results in high bearing stresses and in-plane shear stresses in the carbon-carbon torque tube. Test and analytical results show that the load is not transferred into the torque tube uniformly around the circumference but that most of the load is transferred by four cleats in each row. The load transfer is further complicated by manufacturing clearances between the cleats and the torque tube. Metal shims are placed on both sides of the cleats to reduce the clearances between the cleats and the torque tube.

The disassembled carbon-carbon control surface test component is shown in Figure 4. All of the Rene´ 41 and silicon carbide coated carbon-carbon parts are shown. The four rows of machined cleat holes can be seen on the carbon-carbon torque tube in the background. The control surface is assembled using special tools, shown in the foreground, which are designed to hold the nuts on the back side of the torque tube when attaching the cleats to the Rene´ 41 attachment ring. Figure 5 shows the fully assembled test article without the fibrous insulation. The torque tube, carbon-carbon and Rene´ 41 attachment rings, and the carbon-carbon fasteners are clearly visible. The three hinge fittings at the root would be used to attach the control surface to the supporting wing structure on an actual flight vehicle. However, these fittings attach to test support structure for the structural validation tests.

TEST/ANALYSIS CHALLENGES

The thermal-mechanical testing and finite element analysis of the carbon-carbon control surface pose significant challenges. The structural verification tests require thermal and mechanical loading. The relatively large size of the test article, the need to heat the component to 1649 °C (3000 °F) with simultaneously applied mechanical load, and the requirement to test the component in a purged environment, to prevent oxidation, for temperatures above 427 °C (800 °F), makes the thermal-mechanical testing extremely challenging. Conventional thermocouple attachment techniques are inadequate for use on coated carbon-carbon above 1093 °C (2000 °F). Therefore, infrared pyrometry will be used above 1093 °C (2000 °F) to monitor the elevon outer surface temperature and to provide feedback for real-time thermal control. Silicon carbide coating on carbon-carbon material has significant surface microcracks, which makes it difficult to obtain good room- and elevated-temperature strain measurements.

The finite element analysis assumes a perfect fit-up between the Rene´ 41 cleats and the torque tube which is not realized in the actual structure. A challenge then arises in modeling the torque-tube/attachment-ring joint fit-up accurately. Material property data exist for the carbon-carbon torque tube, however, the present analytical results for the ribs and skins are based on material properties projected from laminate theory. Material property results based on specimens cut from trim pieces and witness panels from the component fabrication will be used in the future.

ROOM-TEMPERATURE TEST APPARATUS AND TECHNIQUES

Instrumentation

A significant amount of instrumentation was required to monitor the control surface's response to load and to ensure its structural integrity during testing. The elevon test required 272 transducers: 246 strain gages, 14 deflection potentiometers, 8 strain-gage bending moment bridges, 2 load cells, and 2 microphones. The strain gages were distributed on the upper and lower skins, all six ribs, the torque tube, and the hinge fittings. The instrumentation placements on the upper and lower skins and ribs are shown in Figure 6. Each rib (Fig. 6(a)) has six strain gages aligned parallel to the skins and two rectangular rosettes located 5.1 cm (2.0 in.) from the rib center-lines. The upper and lower skins (Fig. 6(b)) each have five rectangular rosettes with one located between each rib. Deflections were measured at 14 points on the control surface to determine in-plane and out-of-plane displacements and rotation at the root. Microphones were placed between the center two ribs and in the torque tube to monitor and record any audible structural noises during mechanical loading.

Before testing this full-scale component, NASA LaRC conducted small-scale component tests on a torque-tube/attachment-ring joint segment to determine instrumentation requirements for the full-scale tests and to evaluate analytical techniques [9]. Two strain gages were aligned circumferentially on both sides of each cleat hole and strain-gage rosettes were placed at each cleat hole corner for these small-scale tests. Experience gained from the small-scale tests showed that a significant reduction in the strain-gage density could be made for the full-scale component tests. A plan view of the inner surface of the torque tube and the locations of the strain gages are shown in Figure 7 for the full-scale component test. The torque tube is instrumented with 144 strain gages: 120 on the inner surface and 24 on the outer surface. Strain gages are positioned circumferentially at each cleat hole. There are also gages located at the outer row cleat-hole corners and oriented at 45° (the left-hand and right-hand sides are designated LHS and RHS, respectively). Rectangular rosettes are positioned every 90° around the circumference on the LHS and RHS. These rosettes are mirrored on the outer surface. Figure 8 shows a photograph of the instrumented torque tube for the full-scale test component. The Rene´ 41 bolts and cleats and the instrumentation wire routing can be seen.

Data Acquisition and Control System

Data acquisition, direct digital thermal control, and mechanical profile initiation were accomplished using the Thermostructural Laboratory's Data Acquisition and Control System (DACS) [10]. The system provides real-time visual data analysis displays such as x-y plots, thermal and mechanical control deviation displays, alphanumeric displays, and bar graphs. Figure 9 is a block diagram of the system showing the thermal-mechanical testing of the carbon-carbon control surface. The transducer measurements (strain gage, thermocouple, load cell, etc.) are sent to the analog input sites through the transducer leadwires. This information is then converted from an analog to a digital signal and is sent to a satellite computer which provides real-time analysis monitoring and operational monitoring and control. The main computer system is used to acquire and process data from the satellite system, to provide real-time displays of processed data, and to control the activities of the thermal feedback control and mechanical supervisory control computers. The figure shows separate control loops for thermal and mechanical control. Thermal control is accomplished using the DACS system, whereas mechanical control is accomplished using load controllers. Only the mechanical control loop (shown with a dashed line in Fig. 9) was required for the room-temperature mechanical loading tests. The DACS maximum allowable system measurement error is ± 0.15 percent of reading or $\pm 20\ \mu V$,

whichever is greater. Therefore, for a $\pm 20\ \mu V$ strain measurement input from a single active arm strain gage with a gage factor of 2.0 and a 5 V dc excitation voltage the error band is $\pm 8\ \mu\varepsilon$.

The strain-gage and load cell data for the control surface were recorded on the main DACS while the deflection transducer and microphone data were recorded on a personal computer based data acquisition system. These two data files were then synchronized to a known time standard and were merged post-test.

Test Setup

The carbon-carbon control surface test support structure is shown in Figure 10. This fixture is used to simulate the attachment to a vehicle wing structure and is designed with high stiffness to minimize the overall deflection of the control surface. The support structure is bolted to tie-down tracks in the test area floor. Water cooled fittings are used to attach the control surface to the support structure. These fittings are designed to allow the control surface to thermally expand in-plane and out-of-plane.

Figure 11 is a photograph of the completed room-temperature test setup. A loading mechanism is attached to the control surface at the tip. This mechanism allows for a uniformly distributed load to be applied at the tip in either the up (push-over maneuver) or down (pull-up maneuver) directions. Load is applied with two hydraulic actuators that are each controlled to match a specific mechanical load profile. A 5000-lb load cell is placed between each of the hydraulic actuators and the load bars to measure the applied load. The strain-gage leadwires can be seen routed to the data acquisition system analog input sites in the background.

ROOM-TEMPERATURE ANALYSIS

Two finite element models were created using EAL (engineering analysis language) [11] to analyze the control surface; a course model of the elevon structure and a detailed model of the torque tube. The course model (Fig. 12) consists of the carbon-carbon ribs, facesheets, attachment rings, torque tube, and the Rene´ 41 attachment ring. Only half of the elevon structure was modeled since symmetry conditions were assumed at the vertical mid-plane in line with the ribs. The components of the elevon assembly are joined with beam elements at all bolt locations. In addition, the upper and lower rib sections are offset with beam elements. The uniformly distributed load applied at the control surface tip is transferred from the ribs to the attachment rings. The rings carry the load to the torque tube where it is reacted at the Rene´ 41 attachment ring.

The detailed model of the torque tube (not shown) was used to model the bolt holes and cleat slots accurately. Displacements from the course model were applied to the detailed model of the torque tube. These prescribed displacements were taken from the beam elements in the course model which connect the torque tube to the carbon-carbon and Rene´ 41 attachment rings. Bearing and shear stresses were then determined from the detailed model. Both models were modified during the room-temperature mechanical tests to simulate the actual test conditions more accurately.

ROOM TEMPERATURE TEST AND ANALYSIS CORRELATION

Twenty-five room-temperature mechanical load tests were performed in the up and down directions at load levels building up to 100 percent of the design limit load or 37.77 kN (8490 lb).

Torque Tube Strains

As previously described, the torque-tube/attachment-ring joint is the most critical area of the control surface design. Consequently, there is great interest in the correlation of the torque tube experimental strain data with analysis. Also of great interest is understanding and correcting through redesign, any failure modes observed in the torque tube.

Data from test and analysis of the carbon-carbon torque tube are shown in Figure 13 for the test component loaded to 50-percent design limit load (DLL) in the up and down directions. These results are the diagonal (45°) strains on the bearing face of the cleat holes at the two outermost cleat rows (Fig. 7).

The mechanical load applied at the tip of the test component is transmitted through the torque tube into the Rene´ 41 attachment rings primarily by the cleats located at the 112.5° and 292.5° positions on the torque tube. Therefore, the areas of maximum loading on the torque tube are at the 112.5° and 292.5° positions as shown by the test and analysis data. The trends of the test data correlate very well with the analytical predictions. However, the measured values are generally lower than the predicted values. This difference is caused primarily by the nonideal fit-up between the cleats and the torque tube whereas the analysis assumes a perfect fit-up. The strain value near the cleat located at the 292.5°- position on the LHS of the torque tube for a loading in the down direction is almost twice the analytical prediction. This high-strain value may be caused by this cleat carrying more load than the other cleats in the axial row. The shim on the bearing face for this cleat was removed before proceeding to

the 100-percent design limit load tests. This allowed for load path redistribution and greatly reduced the strain value at that cleat during subsequent tests in the down direction.

Similarly, measured and analytical strain results are shown in Figure 14 for the test component loaded at 100 percent of the DLL in the up and down directions. The high strain value noted in Figure 13 at the 292.5°-position for the LHS down loading is shown in Figure 14 to be considerably reduced due to load path redistribution. This redistribution is a result of the removal of the shim on the bearing face of that cleat. Once again, the highest strain values are near the 112.5° and 292.5° positions for the test and analysis data and the trends of the test data correlated well with the analytical predictions. The magnitudes of the test and analysis data differ possibly due to unknowns in the torque-tube/cleat fit-up with the maximum strains recorded in the up direction at the 292.5°-position on the LHS and RHS. These strains, as seen in Figure 14, are more than twice the analytical values.

The differences between the test and analysis results may be due to the difficulty in obtaining good strain-gage measurements on coated carbon-carbon material. Because of the cracked nature of the coating, relatively large strain gages are required to obtain meaningful measurements. In high-strain gradient areas, the difficulty of positioning the strain gage accurately and the size of the strain gage make it difficult to obtain accurate measurements at a particular point. Also, at loads greater than 80 percent of the DLL, some of the torque-tube/cleat interfaces began to show signs of coating damage which may result in the strain gages measuring the coating strain instead of the carbon-carbon substrate strain.

Upper and Lower Skin Strains

The upper and lower skins are not critical areas of the carbon-carbon elevon design. However, the ability to correlate test data with analytical predictions is essential in developing the thermoelastic analysis techniques used on carbon-carbon structures. Figure 15 shows test and analysis results for the upper and lower skins. These data show the bending strains, parallel with the ribs, on the upper and lower faces at 100-percent DLL in the up and down directions.

The highest strain values occur near the elevon mid-plane. The trends of the test data correlated extremely well with the analysis, however, the magnitude of the test data is consistently lower than the analytical predictions. This may be due to uncertainty in the assumed material properties (i.e., tension and compression modulus) of the upper and lower facesheets. If these properties are too stiff this would cause the experimental strains to be lower than the analytical predictions. Because symmetry is assumed in the finite element analysis, the analytical strain values are identical on both sides of the mid-plane. The test data, however, exhibit slightly unsymmetric behavior about the mid-plane. This behavior is consistent for the upper and lower facesheets and for up and down direction loading.

Tip Deflection

When the control surface returned to an unloaded state after each loading cycle in either the up or down direction, a deflection offset was observed. The magnitude of this post-loading offset reduced after each successive loading cycle in the same direction. Figure 16 is a plot showing tip deflection of the carbon-carbon control surface for the 100-percent DLL cycles in the up and down directions. The pre 100-percent DLL successive post-load offsets are taken into account in this plot. The sign convention for load is positive for a tip load in the down (pull-up maneuver) direction.

The deflection-load curves show an apparent slight increase in stiffness with increasing load. This increased stiffness may be caused by changing load paths in the torque tube as more cleats resist the increasing applied load. The post-load offsets may be caused by the cleats seating against the bearing surface of the cleat hole, crushing of the coating on the bearing face, and, at higher loads, local bearing failures of the torque tube. The offsets were observed to decrease for each additional load cycle in any one direction due to increased mating of the cleats and torque tube. There are several points in the load-deflection curve that show an increase in deflection at a constant load for the 100-percent DLL test in the up direction. These points are load path redistributions caused by local coating or carbon-carbon material failures in the torque tube.

Reversing the load direction requires significantly larger deflections (free play) to reach the test load than were required for subsequent loadings in the same direction. The amount of free play measured for the 100-percent DLL tests in the up and down directions up to 20-percent load was approximately 5.6 cm (2.2 in.). This translates to a free-play angle for a full-scale control surface of ±1.93°. The general rule for control surface free play is to keep the angle less than ±0.25° [12]. The actual free play exceeds the recommended free play for a flight vehicle by a factor of eight. Better fit-up and closer tolerances between the cleats and the bearing surfaces of the torque tube are needed to reduce these large deflections between reversed load cycles.

Coating Damage at 100-Percent Design Limit Load

Figure 17 shows the inner surface of the torque tube with several of the highly loaded cleats removed. This photograph was taken after completing the 100-percent DLL tests in the up and down directions. The coating on the bearing surface of the cleat slot shows evidence of some crushing damage. Removal of the cleat resulted in some spalling of the coating on the inner surface of the torque tube. Several cracks in the coating have also been observed and the coating appears to be disbonded under the strain gage on several of the cleat-hole compression faces. The depth of the cracks and extent of the damage has not been determined.

PLANNED ELEVATED TEMPERATURE TESTING

Instrumentation

The bonded foil strain gages, which were installed for the room-temperature load tests, will also be used for the low-temperature tests to 204 °C (400 °F). No additional strain gages will be installed for this test series. However, additional strain gages will be added to the external surfaces of the test article between the low- and high-temperature test series. These are planned to be free-filament gages applied with a flame spray technique. The expected maximum temperature to which these gages will survive is approximately 1038 to 1093 °C (1900 to 2000 °F). However, to date, useful strain measurements using these free-filament gages have only been made to 816 °C (1500 °F).

Deflection measurements will be made at identical locations to those made during the room-temperature tests. Quartz glass rods will be used to extend the deflection potentiometer cables through the heated area to attachment points on the control surface. The quartz rods will minimize any errors in the deflection measurement caused by thermal expansion of the attachment cables.

Thermocouples (TC) will be added to the control surface before the low-temperature tests. A TC will be installed adjacent to each strain-gage location on the ribs, skins, and attachment fittings, and at many strain-gage locations on the torque tube. Additional TCs will be added to measure temperatures throughout the test article and also to provide feedback for thermal control (Fig. 9). All the TCs attached to carbon-carbon material will be bonded on with a thermally conductive cement. It is anticipated that few of these TC installations will survive much past 1093 °C (2000 °F), if that high. Temperature measurements required for thermal control feedback will be made with noncontact optical-fiber pyrometers. Temperature and structural deflection measurements will be the primary measurements made at test temperatures from 1093 to 1649 °C (2000 to 3000 °F).

Data Acquisition and Control System

The Thermostructural Laboratory's DACS will be used for direct digital thermal control and mechanical profile supervisory control (Fig. 9) for the elevated-temperature testing. Above 1093 °C (2000 °F) optical fiber pyrometers will be used to measure control surface exterior temperatures and provide feedback for thermal control. Research is currently being conducted to integrate these optical pyrometers into the DACS for feedback control. Both control systems shown in Figure 9 will be used during thermal-mechanical testing.

Test Setup

The same test support structure used for the room-temperature tests will also be used for the elevated-temperature tests. A system of infrared quartz lamps will provide heat to the entire upper and lower surfaces of the control surface (Fig. 18) during combined thermal and mechanical loading tests. Insulation on all sides of the test article will minimize thermal losses and protect the support structure and load application hardware from excessive temperatures. Insulation will also be installed around the torque tube and water cooled fittings at the support structure attachment points to maintain those components below the Rene´ 41 design temperature limit of 871 °C (1600 °F).

The first series of elevated temperature testing will be limited to 204 °C (400 °F). Ceramic reflectors with quartz lamps, shown in the right-hand side of Figure 19, will be used in the heating system. These types of reflectors, when used at this relatively low temperature, require no active cooling. At higher temperatures, eventually to 1649 °C (3000 °F), the heater system will consist of high-density quartz lamp reflector units, as shown in the left-hand side of Figure 19. These units require liquid cooling for the polished aluminum reflector housings and gaseous cooling for the lamps, which radiate through quartz glass windows. In each case, the heaters will be divided into thermal control zones so that the test article surface temperature can be tapered downward toward the load introduction hardware and, hence, minimize thermal stresses. The heater systems were designed for easy access to the test article for inspection and instrumentation repair or modification.

Before elevated temperature testing above 427 °C (800 °F), the entire carbon-carbon control surface test setup will be enclosed to enable the test environment to be purged with gaseous nitrogen. The elimination of oxygen during high-temperature tests will preclude any unprotected (uncoated) portions of the carbon-carbon material from oxidizing.

ELEVATED TEMPERATURE ANALYSIS

Thermal and thermal stress analyses were performed during the conceptual design study to assist in the material selection and configuration design. Similar analyses will be conducted for the current control surface configuration to predict the performance of the test component and for comparison with the test results.

Thermal Analysis

The prefabrication thermal analyses for the elevon conceptual design provided peak temperature information for material selection and nodal temperatures for calculating thermal stresses and displacements. All thermal analyses were carried out with the finite difference code SINDA '85 (System Improved Numerical Differencing Analyzer) [13].

The heating rate time histories for the thermal analyses were obtained from radiation equilibrium temperatures associated with proposed vehicle trajectories. An initial set of thermal models was used to verify that the temperature of the Rene´ 41 collars and fasteners would not exceed the 871 °C (1600 °F) design temperature limit. Different types and sizes of insulation and carbon-carbon were used in these analytical trade studies. Simplified boundary conditions were chosen to estimate the heat input into the thermal models. The final design resulted in a maximum use temperature for all of the metal parts below 871 °C (1600 °F) and all of the carbon-carbon parts below the 1649 °C (3000 °F) limit. Subsequent thermal models addressed the heat flux distribution suitable for thermoelastic testing.

The most detailed thermal model addressed the issue of three-dimensional heat transfer between the skin, ribs, torque tube, and fasteners. The temperature distribution obtained from this model was transferred to the finite element structural model as nodal temperatures.

Stress Analysis

Thermal and mechanical loads were incorporated into the preliminary stress analyses. Thermal stresses were avoided in some cases by allowing for differential expansion between some of the Rene´ 41 and carbon-carbon components. The stress-free reference temperature for the carbon-carbon was assumed to be 816 °C (1500 °F), which is close to the pyrolyzation temperature of the ACC parts. A range of stresses were calculated for the elevated temperature tests. These prefabrication stress values will be updated as measured temperature distributions are provided to the thermal stress analysis.

SUMMARY/FUTURE WORK

A carbon-carbon control surface has been defined as the least weight structure for a movable control surface for a NASP generic vehicle. The design and fabrication technology has been demonstrated for this control surface by fabricating a full-scale control surface test component. The structural adequacy of this concept for the hypersonic flight environment is being evaluated through mechanical and thermal-mechanical testing. Twenty-five room-temperature mechanical load tests have been completed up to 100 percent of the design limit load in the up and down directions. The trends of the test results correlated well with finite element analyses. The test results were generally lower than the analytical predictions and indicate that the carbon-carbon torque-tube/attachment-ring joint will transmit the design limit load. However, some damage to the coating on the torque tube occurred for applied loads greater than 80 percent of the design limit load. The full extent of the observed damage has not been determined. The fit-up between the cleats and torque tube is critical to obtaining optimum load transfer between the attachment ring and the torque tube, to minimize the potential for local damage to the torque tube, and also to minimize free play of the control surface.

Eventually, testing of the carbon-carbon control surface will be performed up to 1649 °C (3000 °F) to simulate the thermal environment associated with hypersonic flight. In preparation for these thermal-mechanical tests, the room-temperature finite element analysis model will be refined and the thermal stress analysis of the carbon-carbon control surface will be completed. Temperature measurements and thermal control will be primarily accomplished using infrared pyrometers for the thermal-mechanical test above 1093 °C (2000 °F). Research is currently being conducted to integrate these sensors into the Thermostructural Laboratory's data acquisition and control system for thermal control.

REFERENCES

1. Davis, John G., Jr., *Structures Technology Maturation for NASP*, NASP TM-1017, 1988.

2. Davis, John G., Jr., *Structures Technology Maturation for NASP*, NASP TM-1047, 1989.

3. *Technology Maturation Program, Structures Technology Team*, compiled by Harold N. Murrow, NASP TM-1082, 1988.

4. Davis, John G., Jr. and H.N. Murrow, *Review of Structures Technology Maturation for NASP*, NASP TM-1103, 1990.
5. Sawyer, James Wayne, Philip O. Ransone, and C. W. Stroud, “Carbon-Carbon Development Program for Lightly Loaded Structures,” proceedings of the Third National Aero-Space Plane Technology Symposium, NASA Ames Research Center, Moffett Field, CA, June 2-4, 1987.

6. Ho, T., E. C. Matze, J. Medford, and S. Watabe, *Design Concept Study for NASP Control Surface*, NASA CR-181713, 1988.

7. Ho, T. and J.W. Sawyer, “Design and Fabrication of Carbon-Carbon Control Surface Test Component,” proceedings of the Seventh National Aero-Space Plane Technology Symposium, Naval Post-Graduate School, Monterey, CA, Oct. 23-27, 1989.

8. Sawyer, James Wayne and T.L. Ho, “Development of Carbon-Carbon Control Surface for NASP,” proceedings of the Tenth National Aero-Space Plane Technology Symposium, Naval Post-Graduate School, Monterey, CA, Apr. 23-26, 1991.

9. Sawyer, James Wayne and R. Franklin Vause, “Test and Analysis of Carbon-Carbon Control Surface Torque-Tube/ Attachment-Ring Joint,” proceedings of the Eleventh National Aero-Space Plane Technology Symposium, Naval Post-Graduate School, Monterey, CA, Apr. 21-25, 1992.

10. Zamanzadeh, Behzad, William F. Trover, and Karl F. Anderson, “DACS II - A Distributed Thermal/Mechanical Loads Data Acquisition and Control System,” presented at the International Telemetering Conference/'87, July 1987.

11. Whetstone, W.D., *EISI-EAL Engineering Analysis Language Reference Manual*, Engineering Information Systems Incorporated, San Jose, CA, July, 1983.

12. Norton, William J., *Structures Flight Test Handbook*, AFFTC-TIH-90-001, Air Force Flight Test Center, Edwards Air Force Base, CA, Nov. 1990.

13. Cullimore, B.A., R.G. Goble, C.L. Jensen, and S.G. Ring, “SINDA'85/FLUINT Systems Improved Numerical Differencing Analyzer and Fluid Integrator Version 2.3,” Cosmic Program #MSC-21528, NAS9-17448, Mar. 1990.

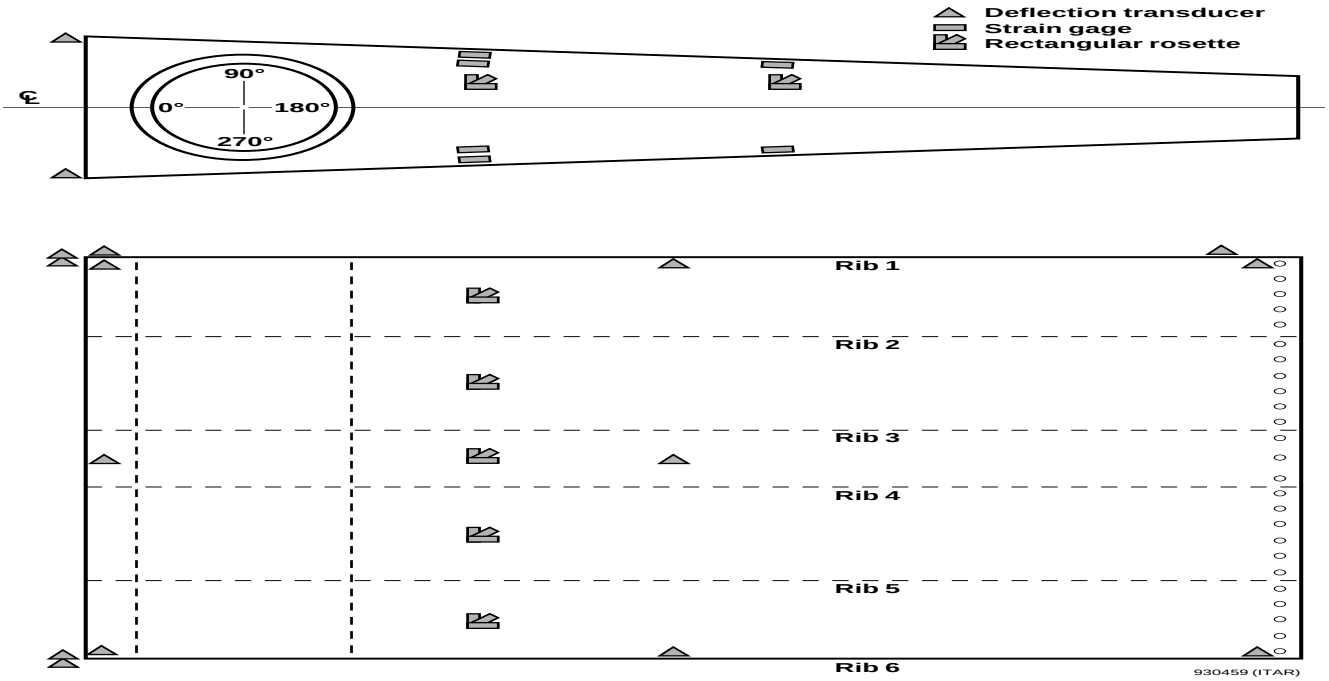

Figure 1. NASP generic vehicle using elevon control surfaces.

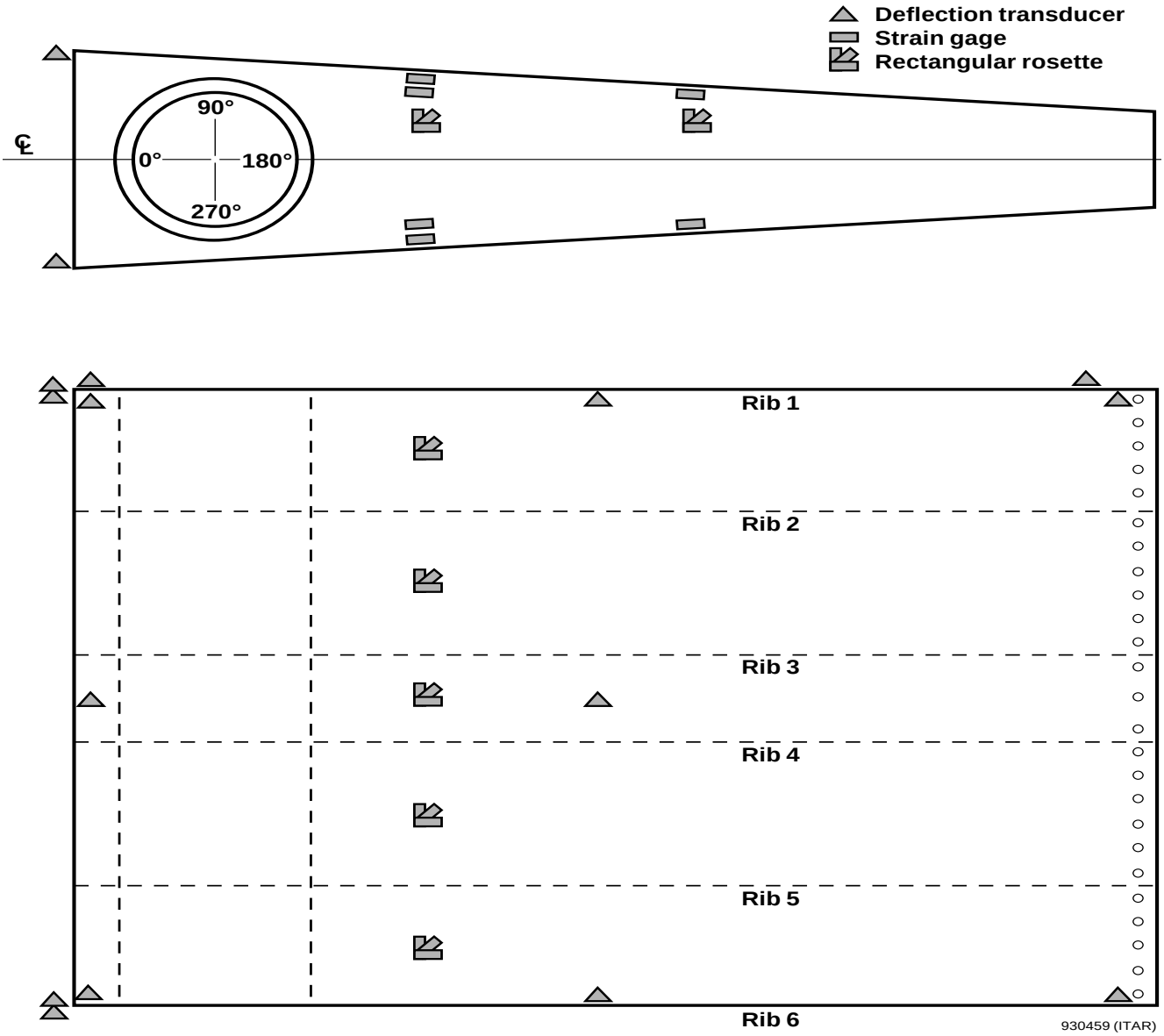

Figure 2. Carbon-carbon control surface assembly drawing.

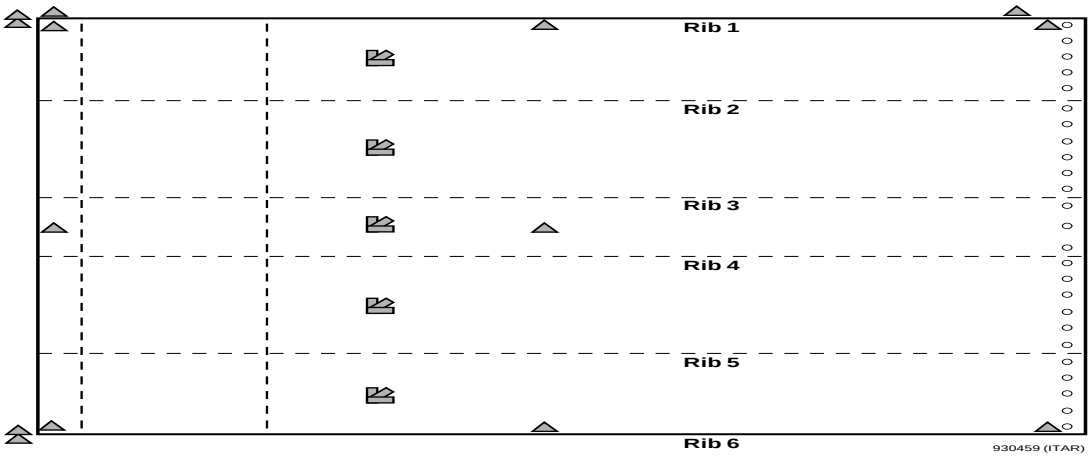

Figure 3. Torque-tube/attachment-ring joint detail.

Figure 4. Disassembled control surface.

Figure 5. Assembled control surface.

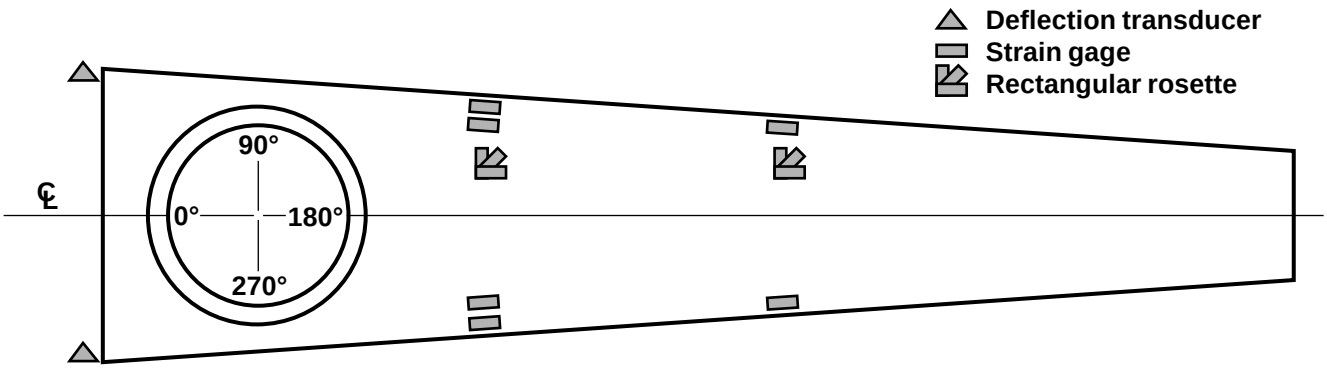

(a) Rib side view.

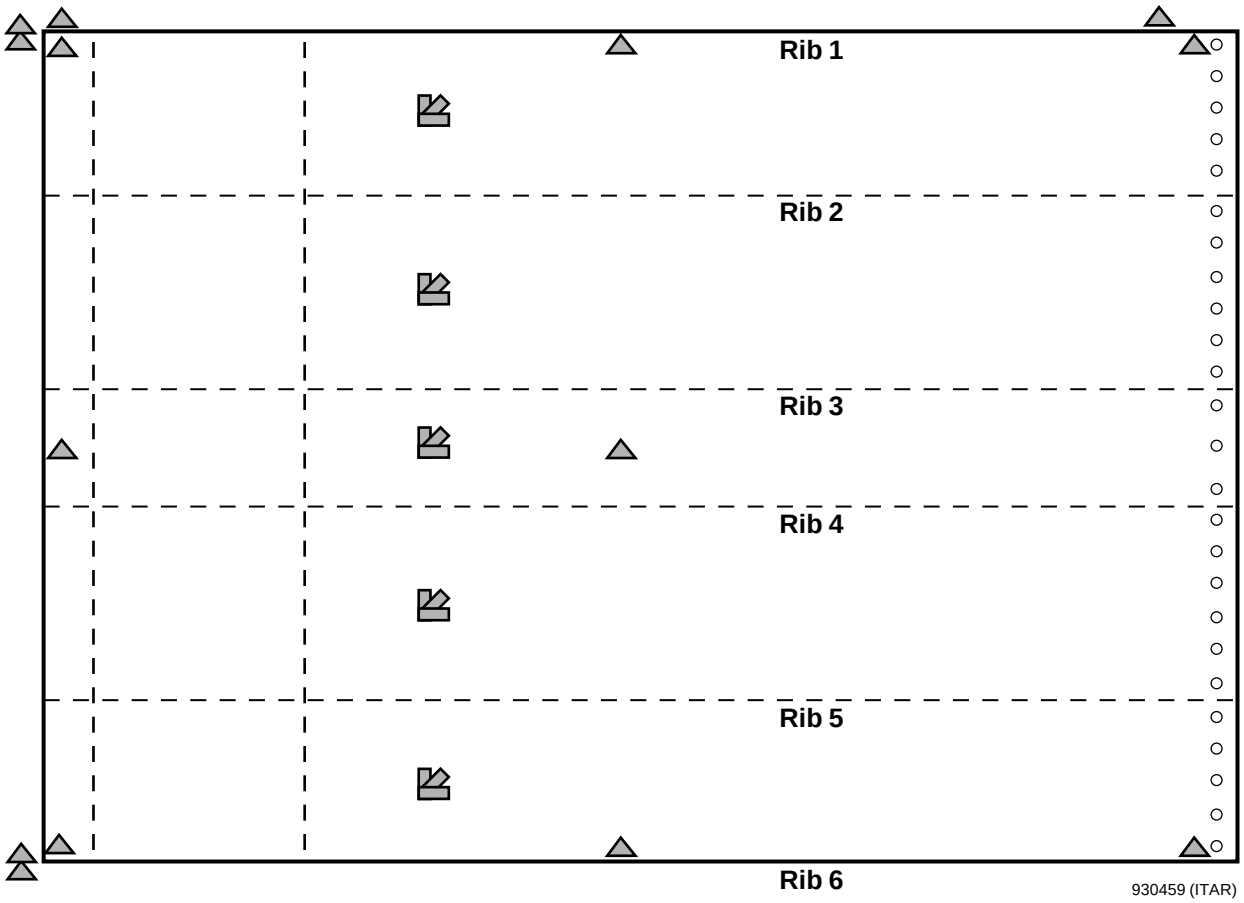

(b) Control surface top view.

Figure 6. Upper and lower skin and rib instrumentation placements.

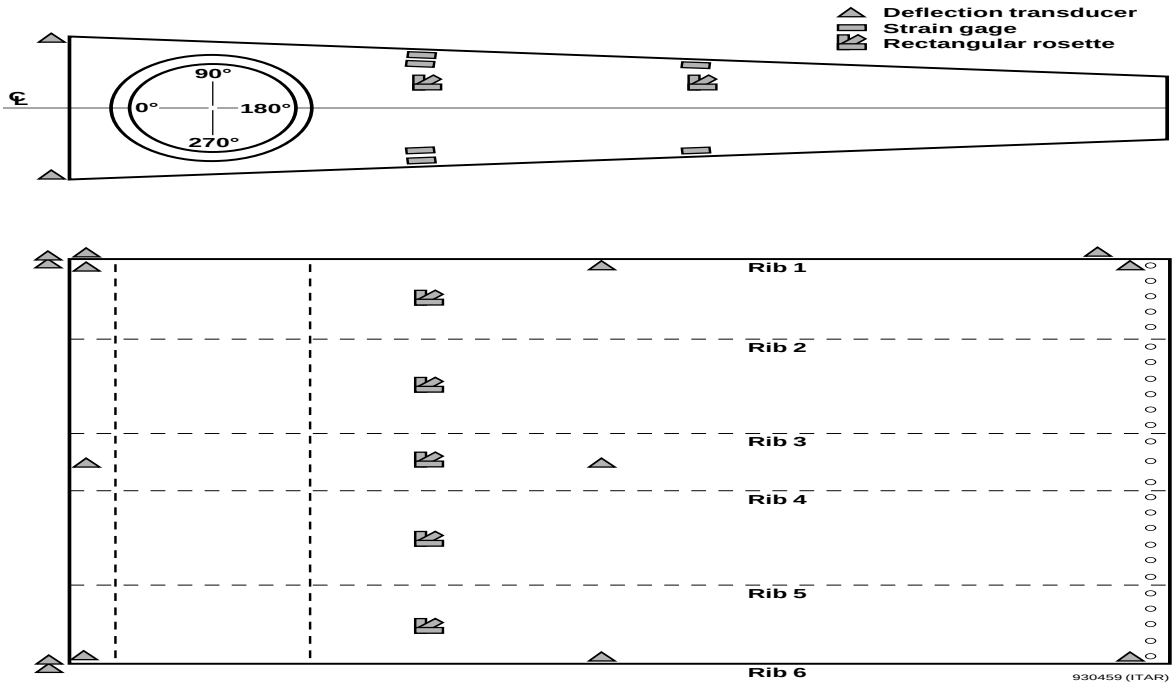

Figure 7. Plan view of the torque tube instrumentation placements.

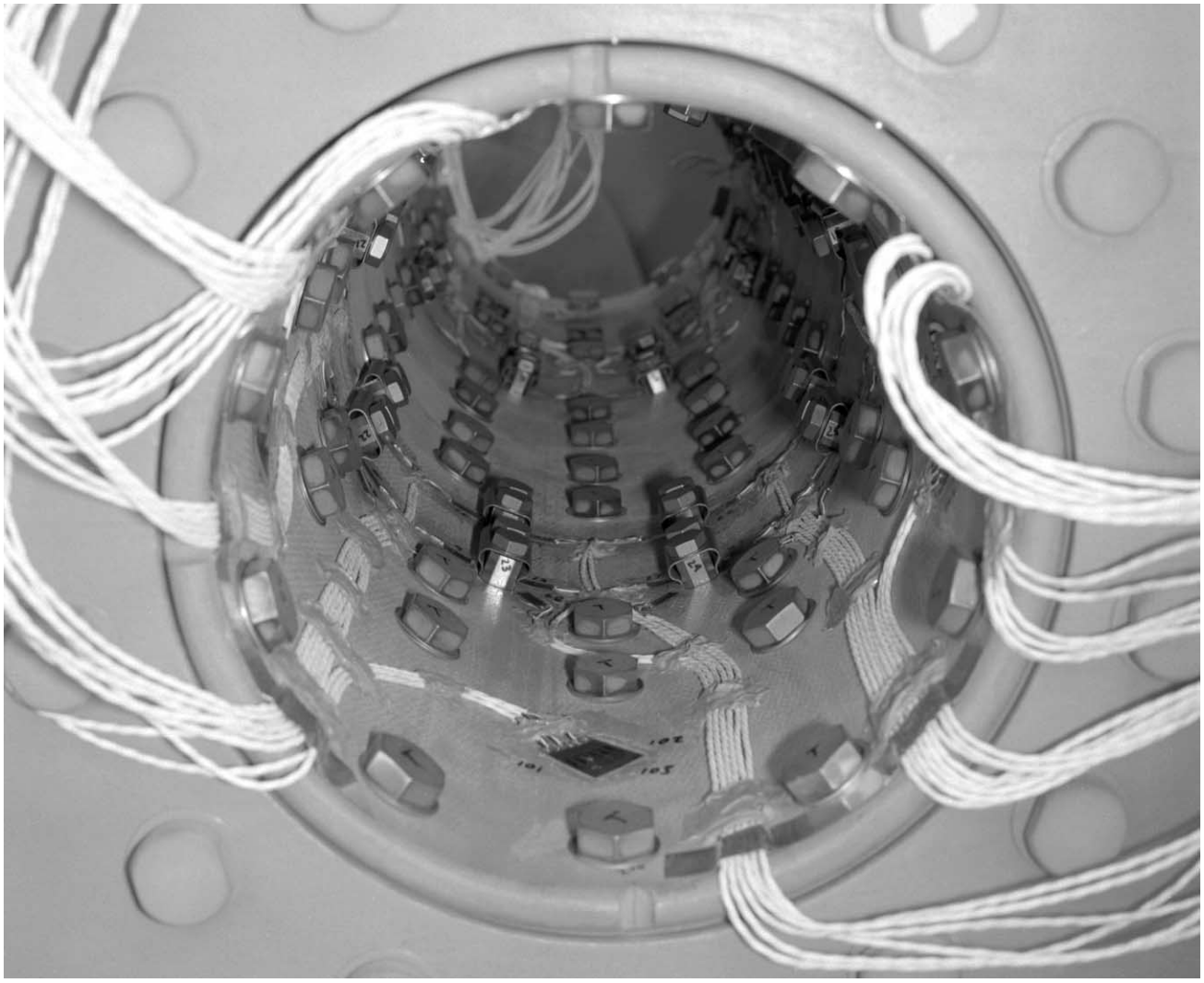

EC92 02041-9

Figure 8. Instrumented torque tube.

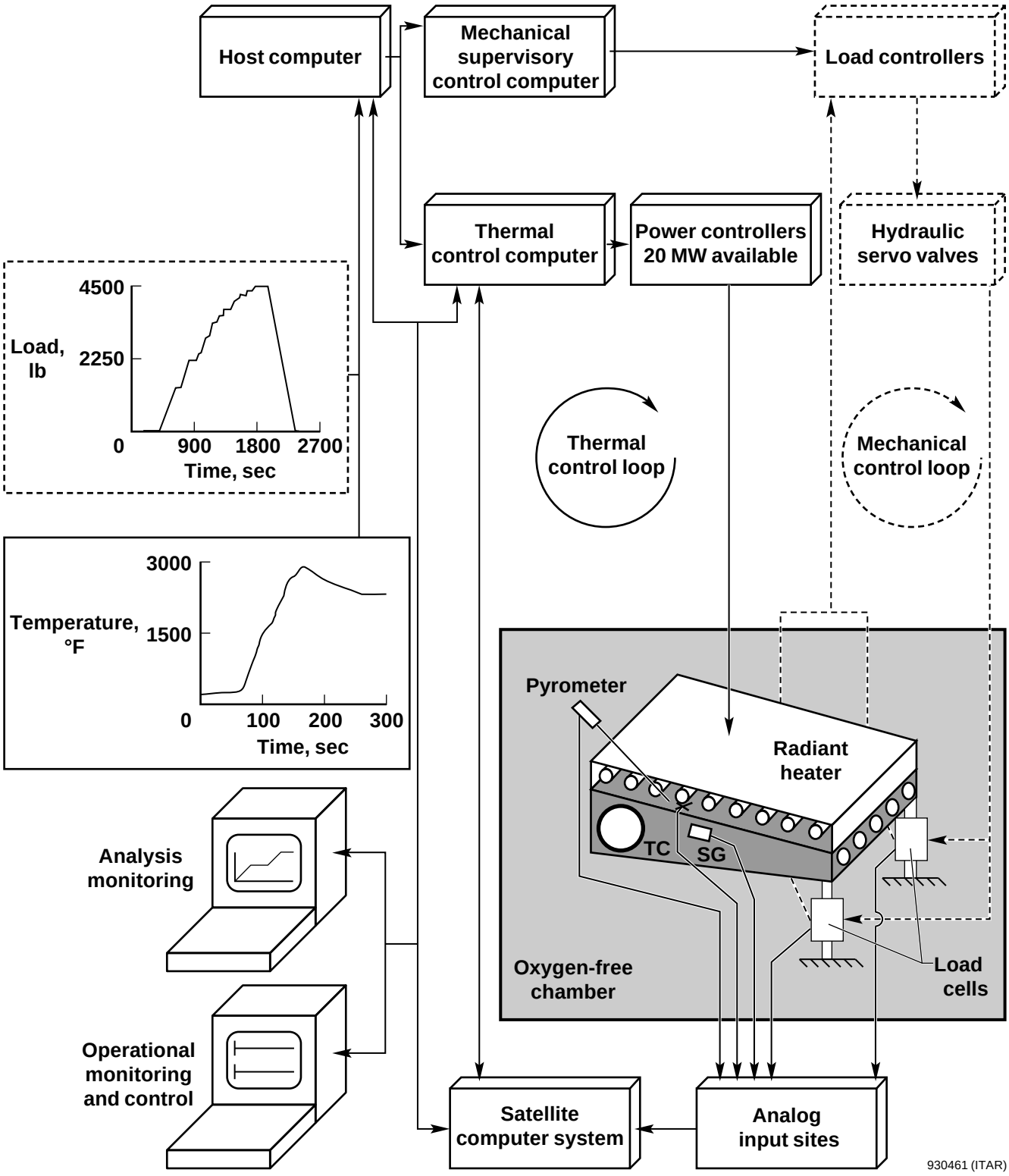

Figure 9. DACS block diagram.

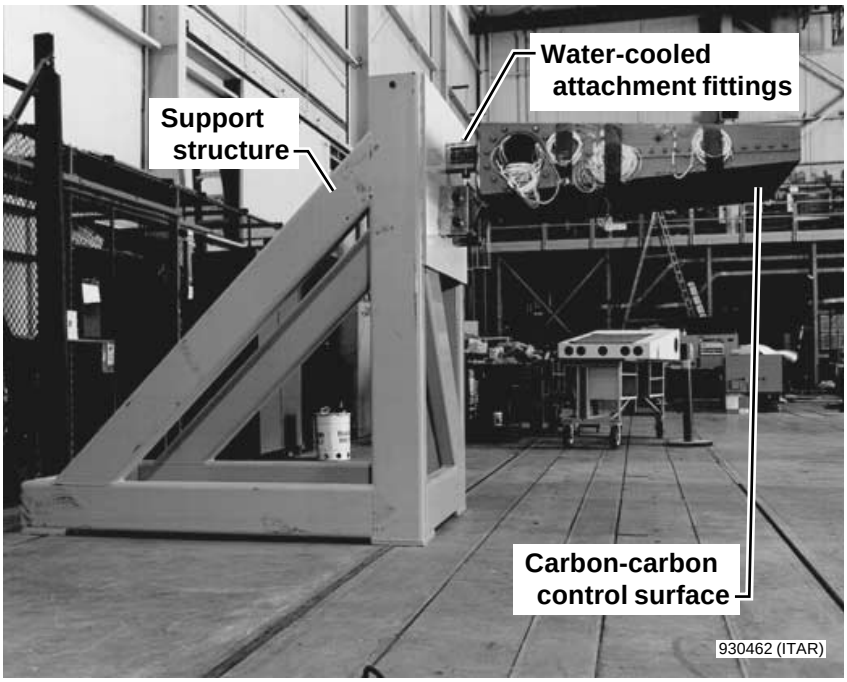

EC92 07014-1

Figure 10. Control surface attached to the support structure.

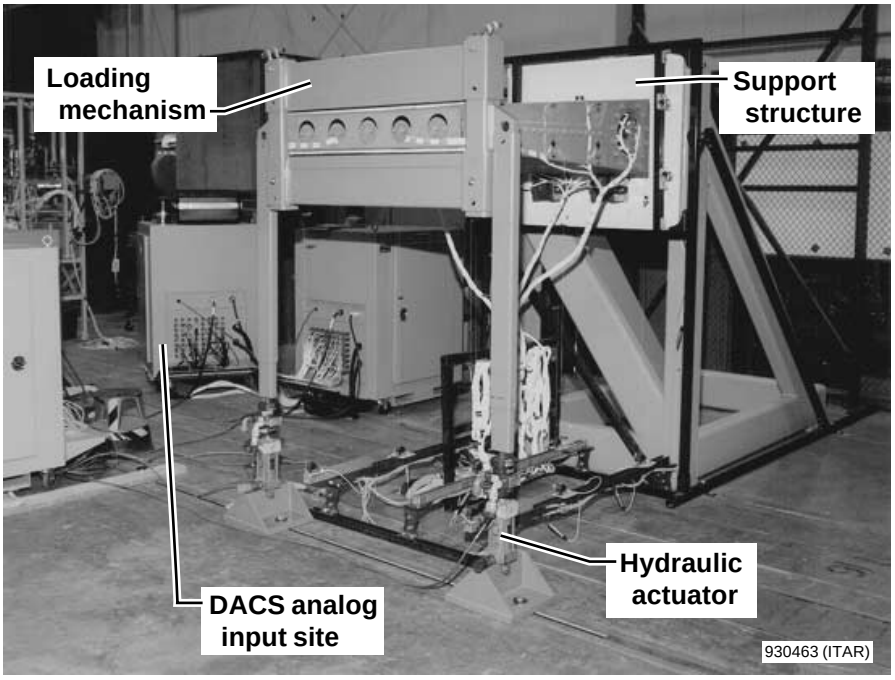

EC92 12012-4

Figure 11. Control surface test setup.

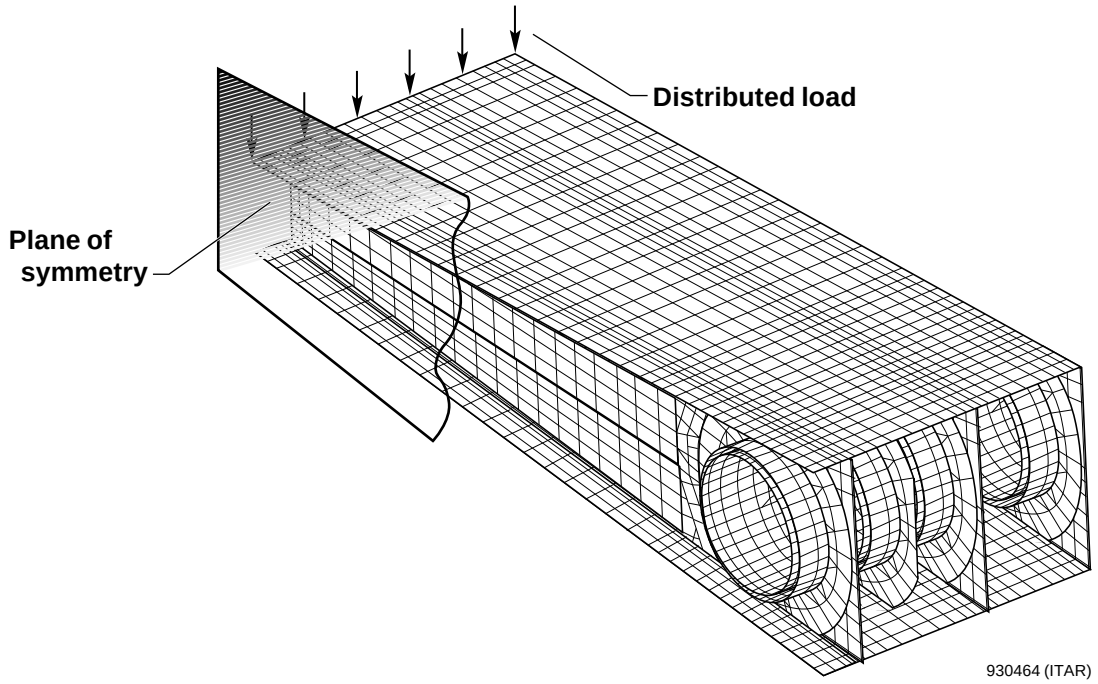

Figure 12. Carbon-carbon control surface finite element analysis.

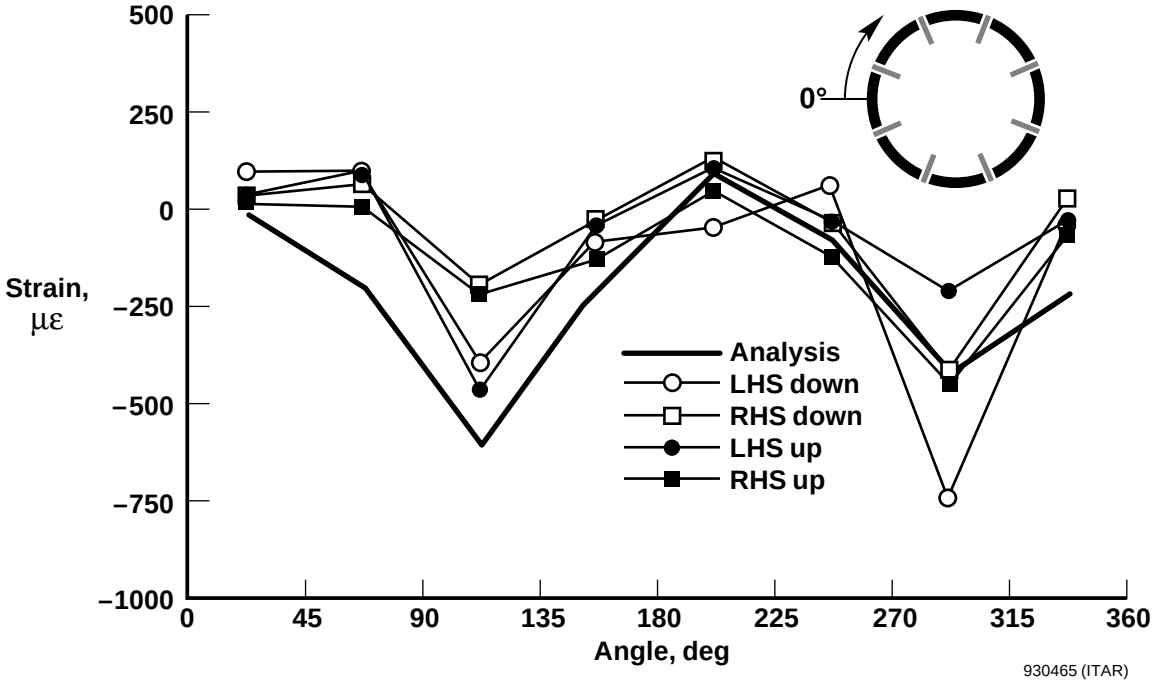

Figure 13. Comparison of test and analysis diagonal strain data at 50-percent design limit load.

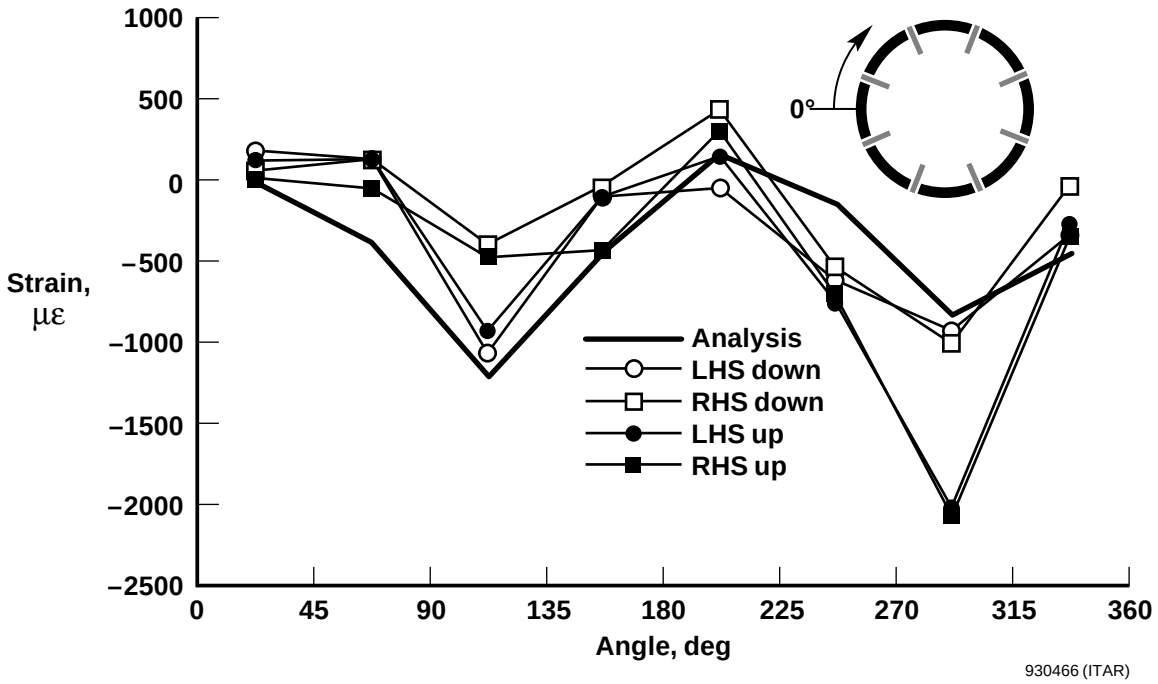

Figure 14. Comparison of test and analysis diagonal strain data at 100-percent design limit load.

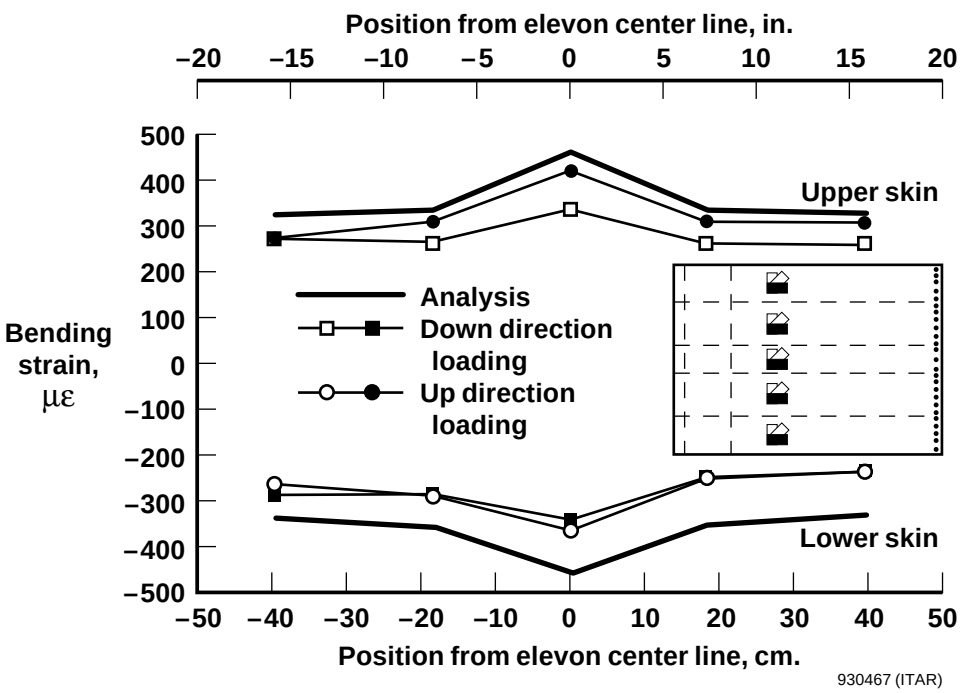

Figure 15. Comparison of test and analysis strain data on the upper and lower skins at 100-percent design limit load.

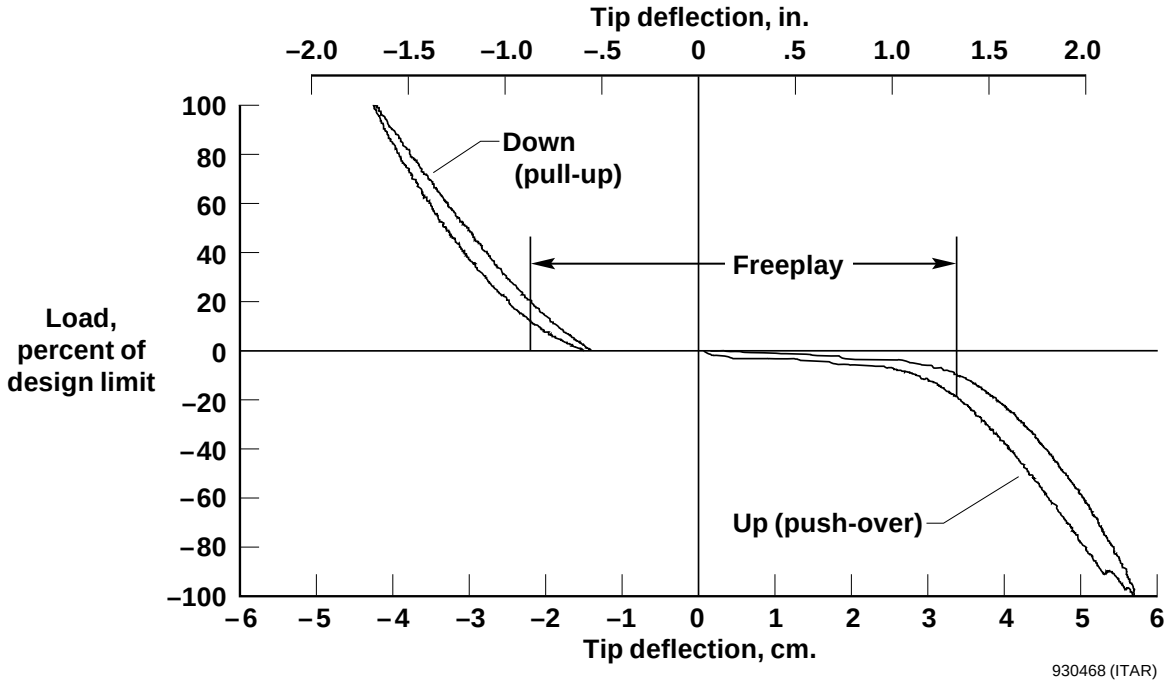

Figure 16. Control surface tip deflection at 100-percent design limit loads.

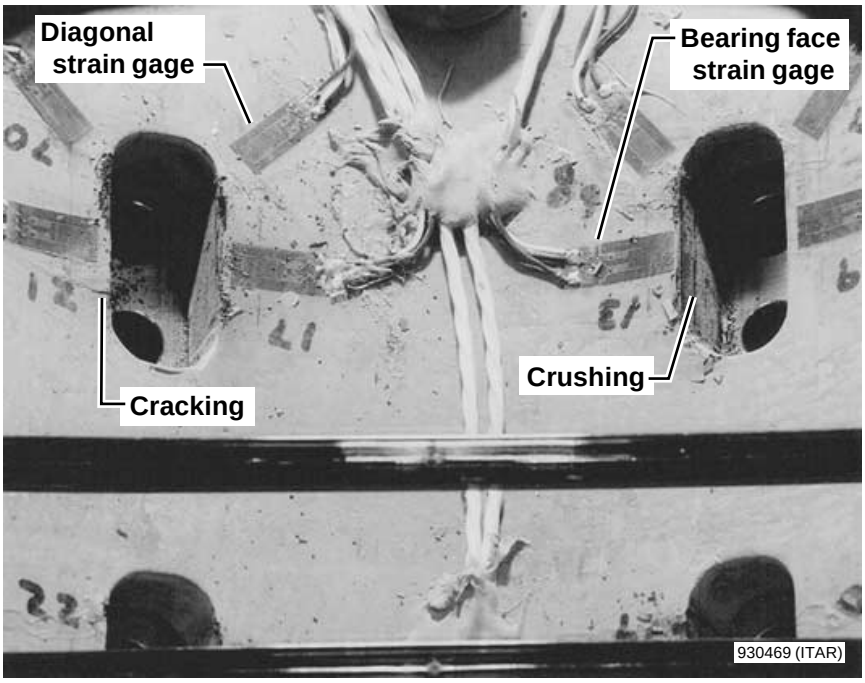

EC93 42023-6

Figure 17. Cleat-hole damage after 100-percent design limit load testing in the up and down directions.

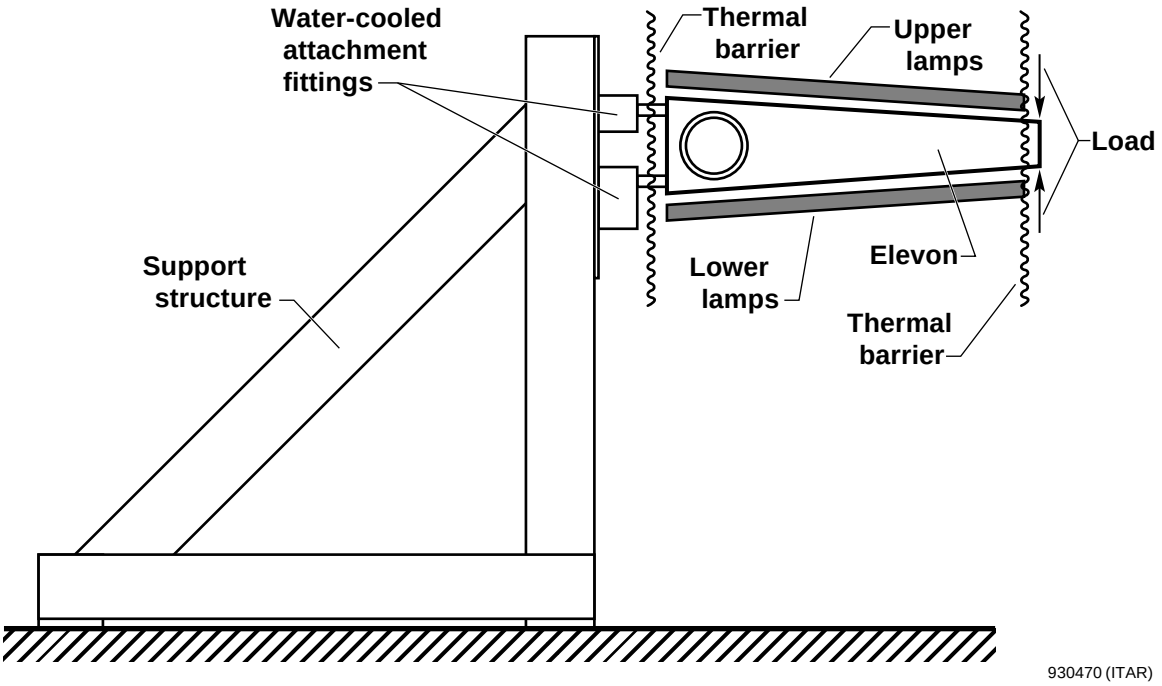

Figure 18. Proposed high-temperature test setup.

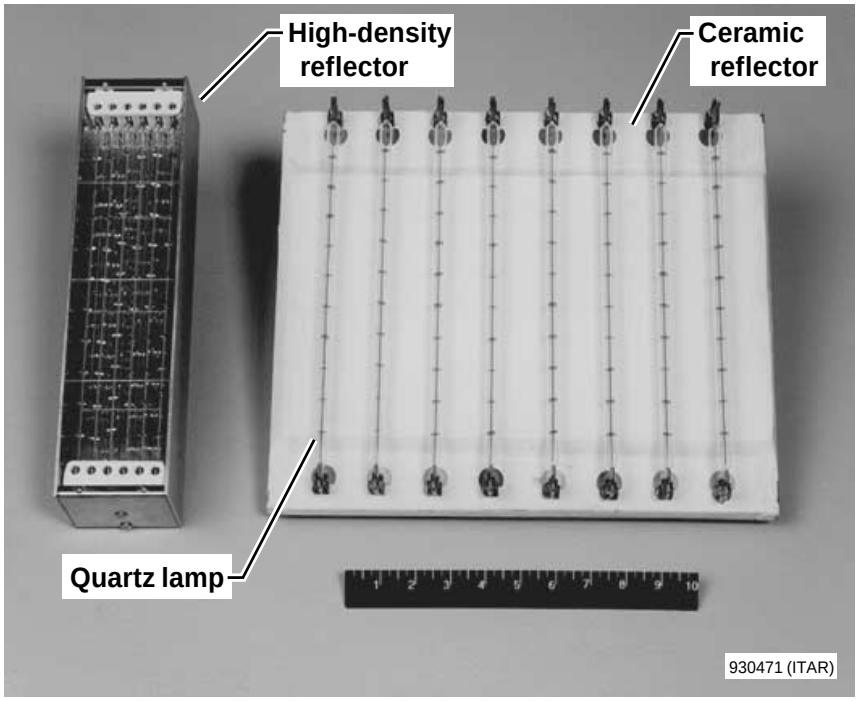

EC93 03183-1

Figure 19. Ceramic and high-density quartz lamp reflectors.